Computer Modeling in Engineering & Sciences CMES, vol.122, no.1, pp.221-234, 2020

Analytic Initial Relative Orbit Solution for Angles-Only Space Rendezvous Using Hybrid Dynamics Method

Baichun Gong[1], Shuang Li[1,*], Lili Zheng[2] and Jinglang Feng[3]

Abstract: A closed-form solution to the angles-only initial relative orbit determination (IROD) problem for space rendezvous with non-cooperated target is developed, where a method of hybrid dynamics with the concept of virtual formation is introduced to analytically solve the problem. Emphasis is placed on developing the solution based on hybrid dynamics (i.e., Clohessy-Wiltshire equations and two-body dynamics), obtaining formation geometries that produce relative orbit state observability, and deriving the approximate analytic error covariance for the IROD solution. A standard Monte Carlo simulation system based on two-body dynamics is used to verify the feasibility and evaluate the performance proposed algorithms. The sensitivity of the solution accuracy to the formation geometry, observation numbers is presented and discussed.

Keywords: Space rendezvous, relative orbit determination, angles-only measurement, covariance analysis.

1 Introduction

Gauss' initial orbit determination problem using angles-only observations is well known. An Earth-based position-known observer gathers line-of-sight angles information (i.e., pairs of azimuth and elevation angles) of a space target over a period time. Theoretically, Gauss' method can be applied to space rendezvous mission when the chaser's positions are known. However, Gauss' method is naturally iterative and has no known closed-form solution [Battin (1987); Curtis (2010)]. Moreover, if the target and chaser are in similar orbits, Gauss' method may be ill-conditioned and suffer from numerical problems.

Analytic solution to the IROD problem may be possible if the linear relative motion dynamics such as Clohessy-Wiltshire (CW) equations [Clohessy and Wiltshire (1960)] are applied. Unfortunately, the angels-only IROD problem during proximity operations suffers from a state observability problem for the short of range measurements [Woffinden and Geller (2009)]. To overcome the observability problem, Chen et al. [Chen and Xu (2011)] proposed

[1] Nanjing University of Aeronautics and Astronautics, Nanjing, 210016, China.

[2] Beijing Institute of Aerospace System Engineering, Beijing, 100076, China.

[3] University of Strathclyde, Glasgow, G11XQ, Scotland.

[*] Corresponding Author: Shuang Li. Email: lishuang@nuaa.edu.cn.

Received: 26 June 2019; Accepted: 03 August 2019.

a two-sensor scheme with double line-of-sight measurements are utilized to solve the IROD problem by using the basic theorem of triangle geometry. Newman et al. [Newman, Lovell, Pratt et al. (2014); Newman, Lovell and Pratt (2014)] successfully applied second-order relative motion models to the IROD problem. Perez et al. [Perez, Geller and Lovell (2018)] established sphere-frame-based dynamics to analyze the angles-only IROD problem, however closed-form solution is still not achieved. Grzymisch et al. [Grzymisch and Ficher (2014)] proposed the orbital maneuver method to improve the state observability. Gaabarri et al. [Gaabarri, Sabatini and Palmerini (2014)] took advantage of the reference image information of the target to solve the angles-only problem. Geller et al. [Klein and Geller (2012); Geller and Klein (2014); Geller and Perez (2015)] demonstrated an angles-only IROD solution for orbital proximity operations by taking advantage of the lever-arm-effect of the offset camera. Gong et al. [Gong, Li, Li et al. (2018)] improved the IROD performance of the lever-arm-effect algorithm. However, this scheme is limited by the fact that the lever-arm cannot be too large for most spacecraft [Gong, Geller and Luo (2016)].

The objectives of this paper are to develop closed-form solution for the angles-only IROD problem during space rendezvous phase based on hybrid dynamics with the concept of virtual distributed, with which no orbital maneuver, double line-of-sight or lever-arm are required. Additionally, the emphasis is also focused on analyzing observable conditions of the orbital state, developing analytic expressions for the IROD state error mean and covariance, evaluating the performance of the IROD algorithm in a standard two-body environment, and determining the better formation geometries which may be potentially used for on-board applications. While contributions due to J_2 and higher-order gravity terms, atmospheric drag, solar radiation pressure are important, these effects are specific to spacecraft orbit selection, mass and geometry, which is beyond the scope of this paper.

The formulation of the IROD problem is presented in Section 2 and its general solution is presented in Section 3. The state observability is analyzed in Section 4 while the linear error covariance analysis for the proposed algorithm is presented in Section 5. The results of Monte Carlo simulation and performance analysis for different formation geometries and measuring conditions are presented in Section 6. Conclusions are presented in Section 7.

2 Problem formulation

Fig. 1 illustrates the formation geometry and vector quantities associated with the IROD problem, where C_v is the virtual chaser which does not have a camera on-board, C_r is the real observer and also named chaser which has a camera mounted in the center of mass. As we can see from the figure, this kind of geometry looks like the case shown in Geller et al. [Geller and Perez (2015)], i.e., the observer C_r seems to be a flying camera offset from the center of mass of chaser C_v and the offset is changing with time. However, it has been deduced that if both of the chaser and offset camera satisfy the CW equations the observability of the orbital state is not possible [Geller and Klein (2014)]. But actually this hypothesis was made under the assumption of the chaser and the camera are close to each other and CW dynamics is used. Thus, in this paper the observability problem will be tried to be solved by the use of nonlinear orbit propagation of the observer C_r.

The same as previous work, the relative motion of the chaser C_r with respect to the target is still governed by the analytic solution to the CW equations in the LVLH (Local Vertical Local Horizontal) reference frame. The origin of a rotating LVLH reference frame is co-located with the target center-of-mass. The axes of the LVLH frame are aligned with the chaser inertial position vector (z-axis or radial), the normal to the orbit plane (y-axis or cross-track), and the along-track direction (x-axis, in the direction of the v-bar or along-track, completes the orthogonal set).

The position of the chaser center-of-mass relative to the target center-of-mass in LVLH coordinates is denoted by $\mathbf{r}(t)$, and the velocity of the chaser relative to the target as observed from a rotating LVLH frame is denoted by $\mathbf{v}(t)$. Vectors without a superscript are assumed to be coordinatized in LVLH coordinates. The motion of the chaser with respect to the target, whether on a flyby orbit, a circumnavigation/football orbit [Woffinden and Geller (2009)], or any other coasting trajectory, is governed by the analytic solution to the CW equations

$$\mathbf{r}(i) = \phi_{rr}(i)\mathbf{r}(0) + \phi_{rv}(i)\mathbf{v}(0)\mathbf{v}(i) = \phi_{vr}(i)\mathbf{r}(0) + \phi_{vv}(i)\mathbf{v}(0) \tag{1}$$

where $\mathbf{r}(0)$, $\mathbf{v}(0)$ are the position and velocity at $t = 0$, $\mathbf{r}(i)$, $\mathbf{v}(i)$ are the position and velocity at time t_i, and $\phi(i)$ is a shorthand notation for transition matrix partition $\phi(t_i - t_0)$.

Moreover, an alternative description of the LOS measurement expressed in the LVLH frame can be given by

$$\mathbf{i}_{los}(i) = \frac{\mathbf{r}(i)}{\|\mathbf{r}(i)\|} \tag{2}$$

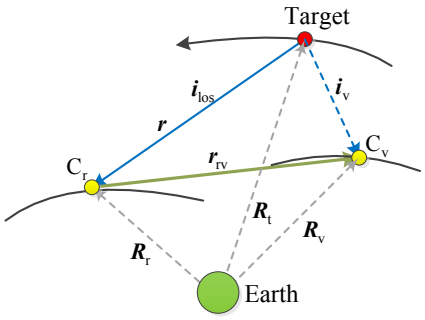

Figure 1: Problem set up and formulation

3 Solution to the angles-only IROD problem

Consider the first LOS observation of Spacecraft C_r, $\mathbf{i}(0)$. The solution for the initial position $\mathbf{r}_v(0)$ and $\mathbf{r}_r(0)$ must satisfy

$$\mathbf{r}_v(0) + \mathbf{r}_{rv}(0) = k_1\mathbf{i}(0) \tag{3}$$

$$\mathbf{r}_r(0) = k_1\mathbf{i}(0) \tag{4}$$

where k_1 is some unknown scale factor of $\mathbf{i}(0)$, and the baseline $\mathbf{r}_{rv}(0)$ is calculated as

$$\mathbf{r}_{\mathrm{rv}}(0) = T_{inertial}^{LVLH}(0)(\mathbf{R}_{\mathrm{r}}(0) - \mathbf{R}_{\mathrm{v}}(0)) \tag{5}$$

where $\mathbf{R}_{\mathrm{v}}(0)$ and $\mathbf{R}_{\mathrm{r}}(0)$ are the inertial position vectors of the Spacecraft $\mathrm{C_v}$ and $\mathrm{C_r}$, $T_{inertial}^{LVLH}$ is the transformation matrix from the inertial frame to LVLH frame. The value of $\mathbf{R}_{\mathrm{r}}$ will be given by on-board GPS receiver, but the value of $\mathbf{R}_{\mathrm{v}}$ (or the orbit of $\mathrm{C_r}$) will be propagated by absolute orbit dynamics with a given initial state $\mathbf{R}_{\mathrm{v}}(0)$ and $\mathbf{V}_{\mathrm{v}}(0)$

$$\begin{cases} \dot{\mathbf{R}}_{\mathrm{v}} = \mathbf{V}_{\mathrm{v}} \\ \dot{\mathbf{V}}_{\mathrm{v}} = \mathbf{g}(\mathbf{R}_{\mathrm{v}}) \end{cases} \tag{6}$$

where $\mathbf{g}$ is the acceleration due to gravity acting on the virtual spacecraft $\mathrm{C_v}$ which is based on a point-mass gravity model [Kaplan (1976)].

Similarly, for the second and third LOS observations the solution for the initial position and velocity $\mathbf{r}_{\mathrm{v}}(0)$, $\mathbf{v}_{\mathrm{v}}(0)$, $\mathbf{r}_{\mathrm{r}}(0)$, $\mathbf{v}_{\mathrm{r}}(0)$ must satisfy

$$\phi_{rr}(1)\mathbf{r}_{\mathrm{v}}(0) + \phi_{rv}(1)\mathbf{v}_{\mathrm{v}}(0) + \mathbf{r}_{\mathrm{rv}}(1) = k_2\mathbf{i}(1) \tag{7}$$

$$\phi_{rr}(1)\mathbf{r}_{\mathrm{r}}(0) + \phi_{rv}(1)\mathbf{v}_{\mathrm{r}}(0) = k_2\mathbf{i}(1) \tag{8}$$

$$\phi_{rr}(2)\mathbf{r}_{\mathrm{v}}(0) + \phi_{rv}(2)\mathbf{v}_{\mathrm{v}}(0) + \mathbf{r}_{\mathrm{rv}}(2) = k_3\mathbf{i}(2) \tag{9}$$

$$\phi_{rr}(2)\mathbf{r}_{\mathrm{r}}(0) + \phi_{rv}(2)\mathbf{v}_{\mathrm{r}}(0) = k_3\mathbf{i}(2) \tag{10}$$

where k_2 and k_3 are also unknown scale factors of $\mathbf{i}(1)$ and $\mathbf{i}(2)$, respectively. Then, when $N \geq 3$ observations are available during a coasting period, the i^{th} observation also satisfies

$$\phi_{rr}(i)\mathbf{r}_{\mathrm{v}}(0) + \phi_{rv}(i)\mathbf{v}_{\mathrm{v}}(0) + \mathbf{r}_{\mathrm{rv}}(i) = k_{i+1}\mathbf{i}(i) \tag{11}$$

$$\phi_{rr}(i)\mathbf{r}_{\mathrm{r}}(0) + \phi_{rv}(i)\mathbf{v}_{\mathrm{r}}(0) = k_{i+1}\mathbf{i}(i) \tag{12}$$

Let $\mathbf{X} = [k_1, \cdots, k_N, \mathbf{r}_{\mathrm{v}}(0)^T, \mathbf{v}_{\mathrm{v}}(0)^T, \mathbf{r}_{\mathrm{r}}(0)^T, \mathbf{v}_{\mathrm{r}}(0)^T]^T$, then the vector Eqs. (3)-(12) represent $6N$ equations with $N+12$ unknowns. Rearranging and writing the result in matrix form produces

$$A\mathbf{X} = \mathbf{B} \tag{13}$$

where

$$A = \begin{bmatrix} \mathbf{i}(0) & 0_{3\times1} & \cdots & 0_{3\times1} & -I_{3\times3} & 0_{3\times3} & 0_{3\times3} & 0_{3\times3} \\ 0_{3\times1} & \mathbf{i}(1) & \cdots & 0_{3\times1} & -\phi_{rr}(1) & -\phi_{rv}(1) & 0_{3\times3} & 0_{3\times3} \\ \vdots & \vdots & \ddots & \vdots & \vdots & \vdots & \vdots & \vdots \\ 0_{3\times1} & 0_{3\times1} & \cdots & \mathbf{i}(N-1) & -\phi_{rr}(N-1) & -\phi_{rv}(N-1) & 0_{3\times3} & 0_{3\times3} \\ \mathbf{i}(0) & 0_{3\times1} & \cdots & 0_{3\times1} & 0_{3\times3} & 0_{3\times3} & -I_{3\times3} & 0_{3\times3} \\ 0_{3\times1} & \mathbf{i}(1) & \cdots & 0_{3\times1} & 0_{3\times3} & 0_{3\times3} & -\phi_{rr}(1) & -\phi_{rv}(1) \end{bmatrix} \tag{14}$$

$$\mathbf{B}=\begin{bmatrix}\mathbf{r}_{\mathrm{rv}}(0)\\ \vdots\\ \mathbf{r}_{\mathrm{rv}}(N-1)\\ \mathbf{0}_{12\times1}\end{bmatrix} \tag{15}$$

Then, the least-squares solution to this set of over-determined equation is

$$\widehat{\mathbf{X}}=(A^TA)^{-1}A^TB \tag{16}$$

After that, unique values for the initial position $\mathbf{r}(0)$ and velocity $\mathbf{v}(0)$ can be extracted.

$$\mathbf{x}_0=\begin{bmatrix}\mathbf{r}(0)\\ \mathbf{v}(0)\end{bmatrix}=C\widehat{\mathbf{X}} \tag{17}$$

where

$$C=\begin{bmatrix}0_{6\times(N+6)} & I_{6\times6}\end{bmatrix} \tag{18}$$

Thus, Eqs. (16)-(17) represents a simple algorithm that can be used to determine the solution to the angles-only IROD problem based on $N\geq3$ observations for any relative motion coasting trajectory, and for any known constant or time-varying chaser orientation.

4 Observability analysis

Conceptually, the relative state $\mathbf{X}$ can be uniquely determined from the measured LOS time history, the angles-only IROD problem is said to be observable. By contrast, it is said to be unobservable if more than one set of states share the same LOS time history. The goal of this section was to analytically analyze the initial relative state's observability criteria of the angles-only IROD problem based on proposed algorithm.

Firstly, as shown in Eq. (5), the baseline $\mathbf{r}_{\mathrm{rv}}$ is calculated from the inertial position of the two spacecraft. But if it is propagated by CW dynamics, i.e.,

$$\mathbf{r}_{\mathrm{rv}}(i)=\phi_{rr}(i)[\mathbf{r}_{\mathrm{r}}(0)-\mathbf{r}_{\mathrm{v}}(0)]+\phi_{rv}(i)[\mathbf{v}_{\mathrm{r}}(0)-\mathbf{v}_{\mathrm{v}}(0)] \tag{19}$$

Then substituting Eq. (19) into Eq. (11) yields

$$\phi_{rr}(i)\mathbf{r}_{\mathrm{r}}(0)+\phi_{rv}(i)\mathbf{v}_{\mathrm{r}}(0)=k_{i+1}\mathbf{i}(i) \tag{20}$$

So when N observations can be obtained, Eq. (13) is reduced to

$$\tilde{A}\mathbf{X}=\mathbf{0} \tag{21}$$

where $\tilde{A}$ is a matrix depending on line-of-sight and transition matrix.

Thus, according to the linear system theorem [Strang (2014)], the unique physical solution cannot be determined from Eq. (21) whatever $\tilde{A}$ is full rank or not, which means unobservable. On contrast, it will be observable if the baseline $\mathbf{r}_{\mathrm{rv}}$ is calculated by Eq. (5). The reason is Eq. (5) stands for the orbital propagation of high-order relative motion dynamics. And as concluded in Woffinden [Woffinden (2008)], the angles-only navigation system will has some observability if the nonlinear dynamics is used. But if spacecraft $\mathrm{C_v}$ and $\mathrm{C_r}$ are so close to each other, e.g., hundreds meters away, Eq. (5) will get a similar

result with CW dynamics which leads to be unobservable. Therefore, it is better to have a longer distance, especially have a larger altitude difference between C_v and C_r in order to improve the observability.

Secondly, as shown in Eq. (13), if column vector $\mathbf{B}$ is zero vector, i.e., $\mathbf{r}_{rv} \equiv \mathbf{0}$, Eq. (13) is homogeneous. Then, the initial orbit cannot be uniquely solved. Thus, the necessary condition for Eq. (13) has unique physical solution is

$$\mathbf{r}_{rv} \not\equiv \mathbf{0} \tag{22}$$

Further, if vector $\mathbf{r}_{rv}$ is parallel to the line-of-sight, the column vector $\mathbf{B}$ is dependent with system state $\mathbf{X}$. Then the initial orbit is unobservable. For example, if there have three observations and

$$\mathbf{r}_{rv}(0) = m\mathbf{r}_r(0) \tag{23}$$

$$\mathbf{r}_{rv}(1) = n\phi_{rr}(1)\mathbf{r}_r(0) + n\phi_{rv}(1)\mathbf{v}_r(0) \tag{24}$$

$$\mathbf{r}_{rv}(2) = k\phi_{rr}(2)\mathbf{r}_r(0) + k\phi_{rv}(2)\mathbf{v}_r(0) \tag{25}$$

where m, n and k are unknown scale factors respectively.

Then the column vector $\mathbf{B}$ can be re-expressed as

$$\mathbf{B} = G\mathbf{X} \tag{26}$$

$$G = \begin{bmatrix} 0_{3\times3} & mI & 0_{3\times3} \\ 0_{3\times3} & n\phi_{rr}(1) & n\phi_{rv}(1) \\ 0_{3\times3} & k\phi_{rr}(2) & k\phi_{rv}(2) \end{bmatrix} \tag{27}$$

Substituting Eq. (26) into Eq. (13) produces

$$(A - G)\mathbf{X} = \mathbf{0} \tag{28}$$

Thus, the initial orbit cannot be solved from Eq. (28) whatever the coefficient matrix $(A-G)$ is full rank or not. As a result, the sufficient and necessary condition of observability is the projection of the baseline $\mathbf{r}_{rv}$ in the LVLH frame cannot be parallel to the line-of-sight, i.e.,

$$\mathbf{r}_{rv} \times \mathbf{i} \not\equiv \mathbf{0} \tag{29}$$

5 Linear error covariance analysis

As shown in Eqs. (13)-(15), the IROD solution requires the knowledge of line-of-sight $\mathbf{i}$ and baseline $\mathbf{r}_{rv}$. The measured values of these variables $\tilde{\mathbf{i}}$ and $\tilde{\mathbf{r}}_{rv}$ contain errors which will lead to estimation errors in the initial relative orbit. Thus, it is very important to figure out how the IROD estimation error and covariance propagate in terms of measurement errors. In the following subsections, the actual measurement models and error models will be built and utilized to do the linear error covariance analysis.

5.1 Measurement models

Firstly, it is assumed that the measured value of the unit LOS vector $\tilde{\mathbf{i}}(j)$ from spacecraft $\mathrm{C_r}$ contains camera measurement error $\boldsymbol{\epsilon}_j$ modeled by zero mean Gaussian noise with a standard deviation $\boldsymbol{\sigma}_{cam}$. The measured value of line-of-sight is given by

$$\tilde{\mathbf{i}}(j) = \left(\mathbf{I} - \left[\boldsymbol{\epsilon}_j \times\right]\right)\mathbf{i}(j) = \mathbf{i}(j) + \left[\mathbf{i}(j)\times\right]\boldsymbol{\epsilon}_j \tag{30}$$

where $[\times]$ is a skew-symmetric cross-product matrix operator and j is a time label.

Secondly, the calculation of the baseline $\tilde{\mathbf{r}}_{\mathrm{rv}}$ requires the inertial-to-LVLH transformation matrix $T_{inertial}^{LVLH}$ and both the inertial positions of spacecraft $\mathrm{C_v}$ and $\mathrm{C_r}$. According to the development of the navigation technologies, errors in the chaser inertial position and velocity vector will be small if there is an average GPS receiver on-board which is very commonly used on low-earth orbital spacecraft. Thus, the position error of $\mathrm{C_r}$ can be modeled by zero mean Gaussian noise with a standard deviation $\boldsymbol{\sigma}_{\mathrm{gps}}$, i.e., $\delta\mathbf{R}_{\mathrm{r}} \sim N(0, \boldsymbol{\sigma}_{\mathrm{gps}}^2)$. Besides, it is supposed that the position error of $\mathrm{C_v}$ is also modeled by a zero mean Gaussian noise with a standard deviation $\boldsymbol{\sigma}_{\mathrm{pos}}$, i.e., $\delta\mathbf{R}_{\mathrm{v}} \sim N(0, \boldsymbol{\sigma}_{\mathrm{pos}}^2)$. Then, the measured baseline $\tilde{\mathbf{r}}_{12}$ can be modeled as follows:

$$\tilde{\mathbf{r}}_{\mathrm{rv}}(j) = \mathbf{r}_{\mathrm{rv}}(j) + T_{inertial}^{LVLH}(j)(\delta\mathbf{R}_{\mathrm{r}j} - \delta\mathbf{R}_{\mathrm{v}j}) \tag{31}$$

As a result of $T_{inertial}^{LVLH}$ is calculated from the estimated inertial position and velocity of $\mathrm{C_v}$ and $\delta\mathbf{R}$ is small, it is assumed that $T_{inertial}^{LVLH}$ is known perfectly and its error can be negligible.

5.2 Analytic error covariance

First of all, the estimation error of initial relative orbit state is given by

$$\delta\mathbf{e} = C\left(\widehat{\mathbf{X}} - \mathbf{X}\right) = C\delta\mathbf{X} \tag{32}$$

where $\widehat{\mathbf{X}}$ denotes the estimation value of the initial state and $\mathbf{X}$ is the true value of the initial state given by

$$\mathbf{X} = A^{+}\mathbf{B} \tag{33}$$

where A^{+} is pseudo-inverse of A.

Letting $\tilde{A} = A + \delta A$, $\widetilde{\mathbf{B}} = \mathbf{B} + \delta\mathbf{B}$, substituting into Eq. (13) and neglecting second-order terms produces

$$\delta\mathbf{X} = A^{+}\left(\delta\mathbf{B} - \delta A A^{+}\mathbf{B}\right) \tag{34}$$

Substituting Eq. (34) into Eq. (32) produces the following expression for the estimation error

$$\delta \mathbf{e} = CA^{+}\left(\delta \mathbf{B} - \delta A A^{+}\mathbf{B}\right) \tag{35}$$

where δA and $\delta \mathbf{B}$ can be obtained by substituting the measurement models into the definition of A and $\mathbf{B}$. Then, these two variables can be expressed as

$$\delta A = H_A \epsilon, \quad \delta \mathbf{B} = H_B \mathbf{v} \tag{36}$$

$$\epsilon = \begin{bmatrix} \boldsymbol{\epsilon}_0 & \cdots & 0_{3\times 1} & 0_{3\times 12} \\ \vdots & \ddots & \vdots & \vdots \\ 0_{3\times 1} & \cdots & \boldsymbol{\epsilon}_{N-1} & 0_{3\times 12} \end{bmatrix}, \mathbf{v} = \begin{bmatrix} \delta \mathbf{R}_{\mathrm{v},0} \\ \delta \mathbf{R}_{\mathrm{r},0} \\ \vdots \\ \delta \mathbf{R}_{\mathrm{v},N-1} \\ \delta \mathbf{R}_{\mathrm{r},N-1} \end{bmatrix} \tag{37}$$

$$H_A = \begin{bmatrix} [\mathbf{i}(0)\times] & 0_{3\times 3} & \cdots & 0_{3\times 3} \\ 0_{3\times 3} & [\mathbf{i}(1)\times] & \cdots & 0_{3\times 3} \\ \vdots & \vdots & \ddots & \vdots \\ 0_{3\times 3} & 0_{3\times 3} & \cdots & [\mathbf{i}(N-1)\times] \\ [\mathbf{i}(0)\times] & 0_{3\times 3} & \cdots & 0_{3\times 3} \\ 0_{3\times 3} & [\mathbf{i}(1)\times] & \cdots & 0_{3\times 3} \end{bmatrix} \tag{38}$$

$$H_B = \begin{bmatrix} T(0) & -T(0) & 0_{3\times 3} & 0_{3\times 3} & \cdots & 0_{3\times 3} & 0_{3\times 3} \\ 0_{3\times 3} & 0_{3\times 3} & T(1) & -T(1) & \cdots & 0_{3\times 3} & 0_{3\times 3} \\ \vdots & \vdots & \vdots & \vdots & \ddots & \vdots & \vdots \\ 0_{3\times 3} & 0_{3\times 3} & 0_{3\times 3} & 0_{3\times 3} & \cdots & T(N-1) & -T(N-1) \\ 0_{6\times 3} & 0_{6\times 3} & 0_{6\times 3} & 0_{6\times 3} & \cdots & 0_{6\times 3} & 0_{6\times 3} \end{bmatrix} \tag{39}$$

where T is a shortcut for the inertial-to-LVLH transformation matrix $T_{inertial}^{LVLH}$.

Substituting Eq. (36) into Eq. (35) yields

$$\delta \mathbf{e} = H_1 \mathbf{v} + H_2 \epsilon A^{+} B \tag{40}$$

where $H_1 = CA^{+}H_B$ and $H_2 = -CA^{+}H_A$. Since the $\boldsymbol{\epsilon}$ and $\mathbf{v}$ are zero mean and uncorrelated, the mean estimation error is given by

$$\mathbf{M} = E[\delta \mathbf{e}] = \mathbf{0}_{6\times 1} \tag{41}$$

and the covariance of the estimation error is given by

$$P = E\left[\left(\delta \mathbf{e} - \mathbf{M}\right)\left(\delta \mathbf{e} - \mathbf{M}\right)^{T}\right] = H_1 \Lambda_0 H_1^{T} + H_2 \Lambda_1 H_2^{T} \tag{42}$$

where the expressions for $\Lambda_0 = E[\mathbf{v}\mathbf{v}^{T}]$ and $\Lambda_1 = E[\epsilon_N \mathbf{X}\mathbf{X}^{T}\epsilon_N^{T}]$ are as the following respectively

$$\Lambda_0 = \begin{bmatrix} \sigma_{\mathrm{pos}}^2 I_{3\times 3} & 0_{3\times 3} & \cdots & 0_{3\times 3} & 0_{3\times 3} \\ 0_{3\times 3} & \sigma_{\mathrm{gps}}^2 I_{3\times 3} & \cdots & 0_{3\times 3} & 0_{3\times 3} \\ \vdots & \vdots & \ddots & \vdots & \vdots \\ 0_{3\times 3} & 0_{3\times 3} & \cdots & \sigma_{\mathrm{pos}}^2 I_{3\times 3} & 0_{3\times 3} \\ 0_{3\times 3} & 0_{3\times 3} & \cdots & 0_{3\times 3} & \sigma_{\mathrm{gps}}^2 I_{3\times 3} \end{bmatrix} \tag{43}$$

$$\Lambda_1 = \sigma_{\text{cam2}}^2 \begin{bmatrix} k_1^2 I_{3\times3} & \cdots & 0_{3\times3} \\ \vdots & \ddots & \vdots \\ 0_{3\times3} & \cdots & k_N^2 I_{3\times3} \end{bmatrix} \tag{44}$$

Although the expressions for the mean and covariance of the estimation error in Eqs. (41)-(42) are expressed in terms of $\mathbf{i}(i)$ and $T_{inertial}^{LVLH}(i)$, in practice, for real-time on-board applications, these expressions will need to be substituted by $\tilde{\mathbf{i}}(i)$ and $\tilde{T}_{inertial}^{LVLH}(i)$.

6 Monte Carlo simulation

A Keplerian two-body dynamics Monte Carlo simulation system is built to verify the validation and evaluate the performance of the proposed algorithm. The truth model state vector for reference is a 12-dimensional vector defined by the inertial state (includes position and velocity) of the two vehicles [Gong, Geller and Luo (2016)]. In the following, the error covariance computational models is presented, the key parameters are set for the simulation and then the performance of the proposed IROD algorithm is analyzed.

6.1 Error covariance computation models

The true estimation error statistics are generated by selecting a fixed set of initial conditions for both spacecraft's inertial state. The truth models generate the spacecraft's trajectories and a LOS time-history. Then the error models in Subsection 3.1 are used to generate a set of observations that are processed by the proposed algorithms to obtain the orbital solution for the ith Monte Carlo run $\hat{\mathbf{x}}_0(i)$. When n Monte Carlo runs are available, the true error mean and covariance for the estimation are calculated by using the following models

$$\mathbf{M}_{true} = \bar{\delta\mathbf{e}} = \frac{1}{n}\sum_{i=1}^{n} \delta\mathbf{e}(i) \tag{45}$$

$$P_{true} = \frac{1}{n-1}\sum_{i=1}^{n} \left[\delta\mathbf{e}(i) - \bar{\delta\mathbf{e}}\right]\left[\delta\mathbf{e}(i) - \bar{\delta\mathbf{e}}\right]^T \tag{46}$$

where the estimation error for the ith Monte Carlo run is $\delta\mathbf{e}(i) = \hat{\mathbf{x}}_0(i) - \mathbf{x}_0$.

Further, it is more intuitive to know how good the range estimate is, because of the well-known range observability problem of angles-only IROD and navigation during orbital proximity operations. Thus, 2-norm will be used to describe the accuracy of the proposed IROD algorithm

$$\begin{cases} M_d = \left\| \dfrac{1}{n}\sum_{i=1}^{n} \delta\mathbf{e}(i) \right\| \\ \sigma_d = \left\| [\sigma_x, \sigma_y, \sigma_z] \right\| \end{cases} \tag{47}$$

where σ_x, σ_y and σ_z are square roots of the first three diagonal elements of P_{true}, i.e., the standard deviation of the error in the x, y, and z directions.

As a result of M_d and σ_d are sufficient to characterize the uncertainties of the relative

range estimate, IROD performance will be measured and presented by M_d and σ_d in the following section.

6.2 Parameters setting

First of all, the emphasis is placed on verifying the proposed IROD algorithm and testing the performances of different distributed formation but not discussing the effect of dynamics, so a circular target orbit is used and the initial orbital elements are as follows: semi-major axis, 6790.15 km; eccentricity, 0.001; inclination, 51.65 degree; ascending node, 281.65 degree; argument of perigee, 37.39 degree; true anomaly, 322.76 degree.

The nominal initial position of virtual chaser C_v is in +v-bar direction and the corresponding velocity is zero, i.e., C_v is initialized as v-bar stationary with respect to the target. The initial relative orbit of C_r will be set in the simulation cases separately.

Secondly, a summary of the other key parameters is provided in Tab. 1. The accuracy of GPS receiver is assumed to be 10 m/axis while the position uncertainty of virtual spacecraft C_v is supposed to be 1 m/axis. And the integration time-step is 1 sec, Monte Carlo runs n is 500 (which can roughly lead to more than 90% confidence), the number of observations N varies from 3 to 21. Additionally, the line-of-sight uncertainty is chosen to medium level, i.e., 0.0001 ran/axis, according to the development of the optical sensor.

Table 1: Key parameters

Parameters	Value	
GPS position uncertainty of C_r	σ_{gps}	10 m/axis
Position uncertainty of C_v	σ_{pos}	1 m/axis
Line-of-sight uncertainty	σ_{cam}	0.0001
Number of Monte Carlo runs	n	500
Number of observations	N	3 to 21
Total simulation time	T_f	3000 s
Integration time-step		1 s

6.3 Angles-only IROD performance analysis

The results of Case 1 are shown in Fig. 2. The initial positions of virtual C_v is 5 km downrange of the target in +v-bar direction. The initial relative position of Chaser C_r is 5 km altitude in the +r-bar direction, and the relative orbit is changed by setting different initial velocity in the direction of along-track while the corresponding velocities are zero in the direction of radial and cross-track. It can be seen that the best estimation is achieved when the initial along-track velocity is zero. Further, the range estimate accuracy can be only several meters if more than 3 observations are available. And the larger the initial along-track velocity is, the worse the estimation is. When the initial along-track velocity is ± 5 m/s and 21 observations are available, M_d is about 1400 m while σ_d is smaller than 20 m. Thus, the estimate error is about 28% of the 5 km initial separation.

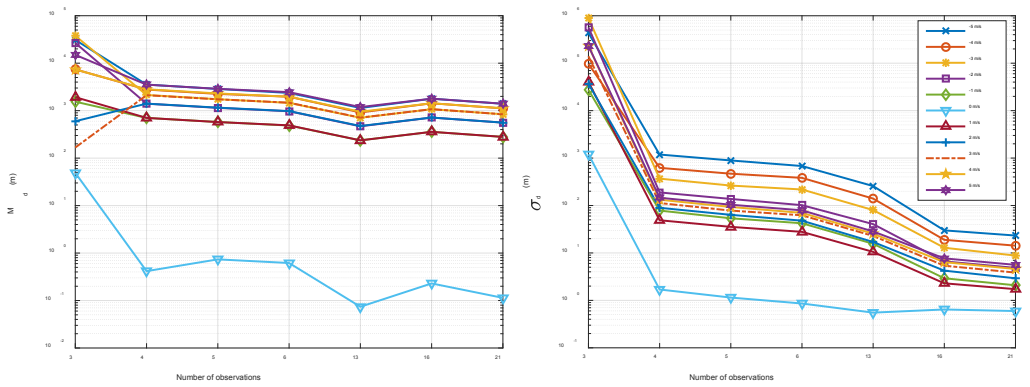

Figure 2: Results of Case 1: Left: error mean; Right: standard deviation

Fig. 3 presents the results for Case 2. In order to make the simulation case being more close to the practical rendezvous circumstance, the chaser is initialized in the position where is 35 km behind and 10 km below the target while the relative velocity is [5.9,0,-0.2] m/s. And the IROD performance will be tested and analyzed by changing virtual spacecraft's orbit. Its nominal initial positions are 1, 5, 15, 50 and 100 km downrange of the target in +v-bar direction, respectively. As shown in Fig. 2, M_d (the estimate error) nearly has no change when the initial virtual position varies from 1 km to 50 km, M_d is around 1600 m (about 4.4% of the initial separation) for 21 observations. M_d becomes smaller that is about 570 m for 21 observations, 1.6% of the initial separation. Further, the vbar stationary position of the virtual spacecraft almost have no influence on the estimate error std which is coincident with the conclusion made by covariance analysis, i.e., the estimate error covariance mainly depends on the level of the absolute positioning noise and LOS measuring noise. It can be seen that σ_d is about 60 m when the number of observations are more than 3.

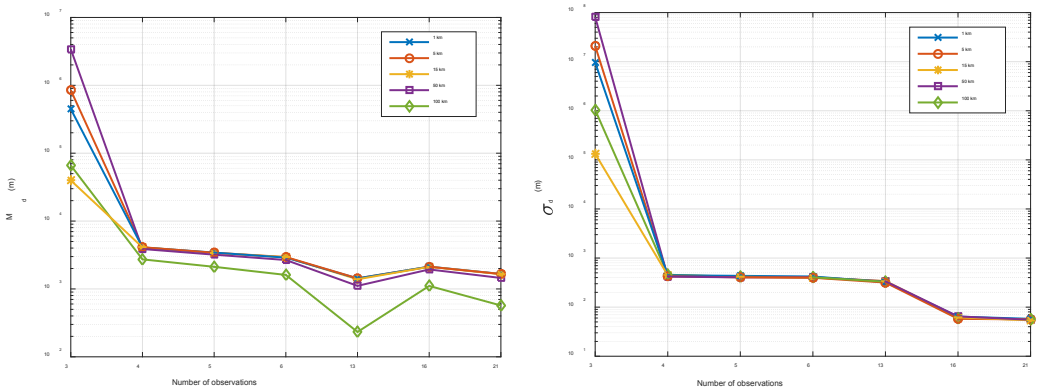

Figure 3: Results of Case 2, Left: error mean; Right: standard deviation

Fig. 4 shows the results for Case 3. In this case, the radial position of the virtual spacecraft

varies from 0 km to 10 km while other conditions are the same with Case 2. It can be seen that the changing of the virtual spacecraft's radial position also has slightly influence on σ_d. However, M_d changed a lot, i.e., about 6 km for the case of 5 km radial position (16.5% of the initial separation) and 18 km for the case of 10 km radial position (49.5% of the initial separation) which are not acceptable. Thus, the virtual spacecraft's v-bar stationary keeping is a good choice for the IROD problem.

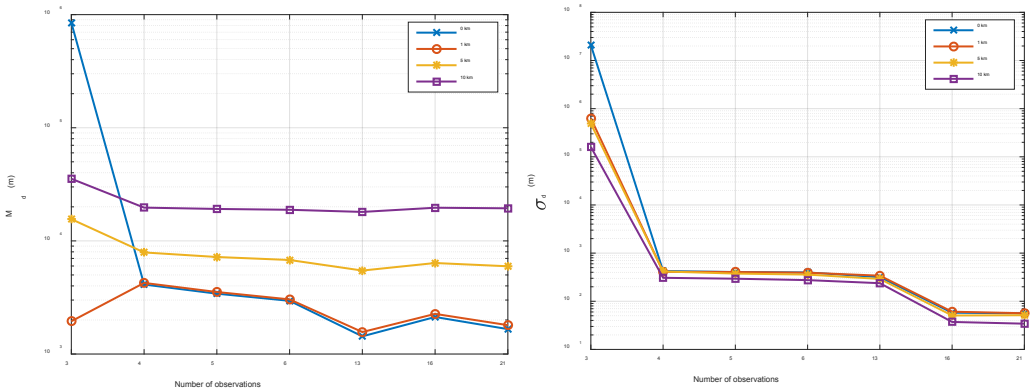

Figure 4: Results of Case 3: Left: error mean; Right: standard deviation

Fig. 5 presents results for Case 4. The virtual spacecraft is initialized to do the oscillating flight along the cross-track direction while other conditions are the same with Case 2. The oscillating magnitude varies from 0 km to 100 km. And the initial position of the virtual spacecraft is 5 km downrange of the target in the +vbar direction. Again, σ_d shows the same trend with those of Cases 2 and 3. And it can be seen that the change of the oscillating magnitude has slight impact on the range estimation, i.e., when the oscillating magnitude increases, the estimate error increases a little bit. Therefore, it is better to assume the virtual spacecraft is co-planar with the target.

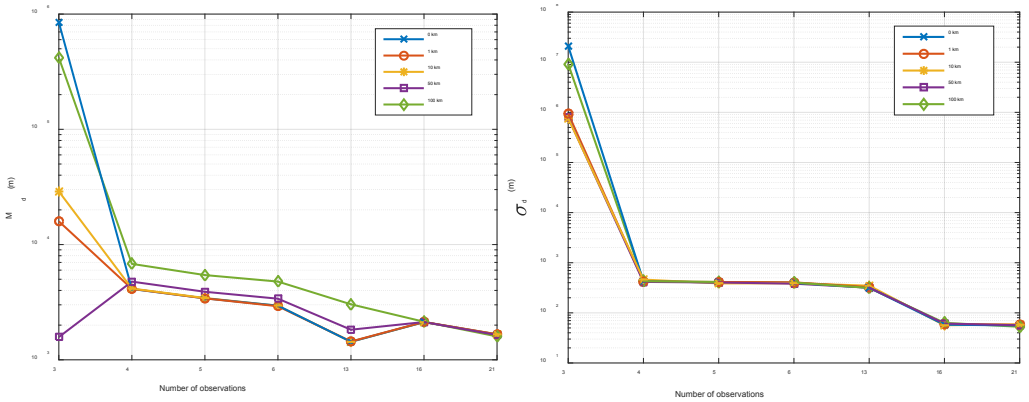

Figure 5: Results of Case 4: Left: error mean**;** Right: standard deviation

7 Conclusions

This paper presented a hybrid dynamics scheme with the concept of virtual distribution to analytically determine the initial relative orbit for angles-only rendezvous mission. Observable condition and approximately closed-form estimate error covariance were obtained by observability analysis and linear covariance analysis in the context of Clohessy-Wiltshire equations. And the detailed performance analysis of the proposed IROD algorithm was conducted and presented based on standard two-body Monte Carlo simulations and classical rendezvous missions. The simulation results has shown the possible potential of the proposed algorithm to analytically solve the angles-only IROD problem for rendezvous mission.

Acknowledgement: This work is supported in part by the Natural Science Foundation of China (11802119), the National Postdoctoral Program for Innovative Talents (BX201700304), and Fundamental Research Funds for Central Universities (NT2019023).

Conflicts of Interest: The authors declare that they have no conflicts of interest to report regarding the present study.

References

Battin, R. H. (1987): *An Introduction to the Mathematics and Methods of Astrodynamics*, pp. 131-140. New York: AIAA.

Chen, T.; Xu, S. (2011): Approach guidance with double-line-of-sight-measuring navigation constraint for autonomous rendezvous. *Journal of Guidance, Control and Dynamics*, vol. 34, pp. 678-687.

Clohessy, W. H.; Wiltshire, R. (1960): Terminal guidance system for satellite rendezvous. *Journal of the Aero/Space Sciences*, vol. 27, no. 3, pp. 653-658.

Curtis, H. D. (2010): *Orbital Mechanics for Engineering Students*. New York: Elsevier.

Gasbarri, P.; Sabatini, M.; Palmerini, G. (2014): Ground tests for vision based determination and control of formation flying spacecraft trajectories. *Acta Astronautica*, vol. 102, pp. 378-391.

Geller, D. K.; Klein, I. (2014): Angles-only navigation state observability during orbital proximity operations. *Journal of Guidance, Control and Dynamics*, vol. 37, no. 6, pp. 1976-1983.

Geller, D.; Perez, A. (2015): Initial relative orbit determination for close-in proximity operations. *Journal of Guidance, Control, and Dynamics*, vol. 38, no. 9, pp. 1833-1842.

Gong, B. C.; Li, W. D.; Li, S.; Zheng, L. L. (2018): Angles-only initial relative orbit determination algorithm for noncooperative spacecraft proximity operations. *Astrodynamics*, vol. 2, no. 3, pp. 217-231.

Gong, B. C.; Geller, D.; Luo, J. J. (2016): Initial relative orbit determination analytical covariance and performance analysis for proximity operations. *AIAA Journal of Spacecraft and Rockets*, vol. 53, no. 5, pp. 822-835.

Grzymisch, J.; Ficher, W. (2014): Observability criteria and unobservable maneuvers for in-orbit bearings-only navigation. *Journal of Guidance, Control and Dynamics*, vol. 37, no. 4, pp. 1250-1259.

Kaplan, M. H. (1976): *Modern Spacecraft Dynamics and Control*. pp. 343-370, Wiley, New York.

Klein, I.; Geller, D. (2012): Zero delta-V solution to the angles-only range observability problem during orbital proximity operations. *Itzhack Y. Bar-Itzhack Memorial Symposium*, Haifa, Israel.

Newman, B.; Lovell, A.; Pratt, E.; Duncan, E. (2014): Quadratic hexa-dimensional solution for relative orbit determination. *AIAA/AAS Astrodynamics Specialist Conference*, San Diego, California.

Newman, B.; Lovell, A.; Pratt, E. (2014): Second order nonlinear initial orbit determination for relative motion using Volterra theory. *Proceedings of the AAS-AIAA Space Flight Mechanics Meeting*, Santa Fe, New Mexico.

Perez, A. C.; Geller, K. D.; Lovell, T. A. (2018): Non-iterative angles-only initial relative orbit determination with perturbations. *Acta Astronautica*, vol. 151, pp. 146-159.

Strang, G. (2014): *Linear Algebra and Its Applications*. Elsevier Science.

Woffinden, D. C.; Geller, D. K. (2009): Observability criteria for angles-only navigation. *IEEE Transactions on Aerospace and Electronic Systems*, vol. 45, no. 3, pp. 1194-1208.

Woffinden, D. (2008): *Angles-Only Navigation for Autonomous Orbital Rendezvous (Ph.D. Thesis)*. Utah State University.